Nonlinear Dyn (2017) 87:851–862
DOI 10.1007/s11071-016-3083-8

ORIGINAL PAPER

Solitons and dromion-like structures in an inhomogeneous optical fiber

Jin-Wei Yang · Yi-Tian Gao · Yu-Jie Feng · Chuan-Qi Su

Received: 11 May 2016 / Accepted: 9 September 2016 / Published online: 1 October 2016

Abstract In this paper, a generalized higher-order variable-coefficient nonlinear Schrödinger equation is studied, which describes the propagation of subpicosecond or femtosecond pulses in an inhomogeneous optical fiber. We derive a set of the integrable constraints on the variable coefficients. Under those constraints, via the symbolic computation and modified Hirota method, bilinear equations, one-, two-,three-soliton solutions and dromion-like structures are obtained. Properties and interactions for the solitons are studied: (a) effects on the solitons resulting from the wave number k, third-order dispersion $\delta_1(z)$, group velocity dispersion $\alpha(z)$, gain/loss $\Gamma_2(z)$ and group-velocity-related $\gamma(z)$ are discussed analytically and graphically where z is the normalized propagation distance along the fiber; (b) bound state with different values of $\alpha(z)$, $\delta_1(z)$, $\gamma(z)$ and $\Gamma_2(z)$ are presented where some periodic or quasiperiodic formulae are derived. Interactions between the two solitons and between the bound states and a single soliton are, respectively, discussed; and (c) single, double and triple dromion-like structures with different values of $\alpha(z)$, $\delta_1(z)$, $\gamma(z)$ are also presented, distortions of which are found to be determined by those variable coefficients.

J.-W. Yang · Y.-T. Gao (✉) · Y.-J. Feng · C.-Q. Su
Ministry-of-Education Key Laboratory of Fluid Mechanics and National Laboratory for Computational Fluid Dynamics, Beijing University of Aeronautics and Astronautics, Beijing 100191, China
e-mail: gaoyt163@163.com

Keywords Optical fiber · Higher-order variable-coefficient nonlinear Schrödinger equation · Hirota's bilinear method · Symbolic computation · Dromion-like structures · Solitons

1 Introduction

Soliton study has been seen in fluids [1–8], plasmas [9–11], Bose–Einstein condensations [12–15], biophysics [16,17] and fiber communication systems [18–21]. In order to derive the soliton solutions for nonlinear evolution equations, the Hirota's bilinear method has been reported, which plays an important role in soliton theory [22,23]. As application of the Horita's bilinear method, many analytical solutions for some nonlinear evolution equations have been constructed [24–31]. Furthermore, the Hirota's bilinear method has been generalized [32] and a refined invariant subspace method has been systematically presented and analyzed for solving nonlinear equations [33,34]. Nonlinear Schrödinger (NLS) equation with the group velocity dispersion (GVD) and self-phase modulation (SPM) [35,36],

$$i\Omega_x + \frac{1}{2}\Omega|\Omega|^2 + \Omega_{\tau\tau} = 0, \tag{1}$$

is a model for the propagation and interaction of optical solitons in the picosecond domain, where x and τ, respectively, are the normalized propagation distance along the fiber and the retarded time, $\Omega(x, \tau)$ is the slowly varying envelope of the electric field, and the subscripts represent the partial derivatives. Optical solitons in a dielectric fiber have been regarded as an alternative data bit carrier to the next generation of ultrafast optical telecommunication systems [37,38]. A systematic study for Eq. (1) has been reported in [39]. For the inhomogeneous optical fiber, the subpicosecond or femtosecond soliton pulses can be governed by the following higher-order variable-coefficient NLS equation [40–42]:

$$\begin{aligned} &iu_z + \alpha(z)u_{tt} + \beta(z)u|u|^2 + i\gamma(z)u_t \\ &\quad + i\delta_1(z)u_{ttt} + i\delta_2(z)(u|u|^2)_t + i\delta_3(z)u(|u|^2)_t \\ &\quad + [\Gamma_1(z) + i\Gamma_2(z)]u = 0, \end{aligned} \tag{2}$$

where z and t are the normalized propagation distance along the fiber and retarded time, $u(z,t)$ represents the complex envelope of the electric field in the comoving frame, all of the variable coefficients are the real functions of z, $\alpha(z)$ and $\beta(z)$ denote the GVD and SPM, respectively, the term proportional to $\gamma(z)$ results from the group velocity, $\Gamma_1(z)$ is the frequency shift parameter, $\Gamma_2(z)$ is the linear gain/loss, $\delta_1(z)$ denotes the third-order dispersion (TOD), $\delta_2(z)$ is the self-steepening (SS), and $\delta_3(z)$ is related to the delayed nonlinear response effect.

In general, Eq. (2) is not integrable [43–45]. Two sets of the integrable constraints for Eq. (2) via the Painlevé analysis have been reported [41], one of which, $\alpha(z) = -3\beta(z)\delta_1(z)/\delta_3(z)$ and $\delta_3(z) = q_1\delta_1(z)e^{2\int(\Gamma_2(z)\mathrm{d}z)}$ where q_1 is a constant, is similar to that shown in Refs. [45–47]. Under the other set, $\alpha(z) = -3q_2\delta_1(z)/(2c_3)$ and $\delta_3(z) = q_3\delta_1(z)$ $e^{2\int(\Gamma_2(z)\mathrm{d}z)}$ where $q_2 \neq 0$ and $q_3 \neq 0$ are a couple of constants, the 2×2 Lax pair has been transformed to a 3×3 linear eigenvalue problem with some soliton solutions obtained via the Darboux transformation [41,48]. Anti-dark solitons for Eq. (2) have been constructed [42].

Special cases of Eq. (2) in the optical fibers have been seen: (a) When $\alpha(z) = d_0(z)/2$, $\beta(z) = h_0(z)$, $\delta_1(z) = b_0(z)/6, \delta_2(z) = -l_0(z), \delta_3(z) = -ik_0(z)$ and $\gamma(z) = \Gamma_1(z) = \Gamma_2(z) = 0$, Eq. (2) can be reduced to a perturbed NLS equation which describes the long distance propagation for the very short optical solitons in a nonlinear optical fiber, where $d_0(z)$ and $b_0(z)$ are the second-order and third-order dispersion profiles between the amplifiers, and $h_0(z)$, $k_0(z)$ and $l_0(z)$ are chosen to incorporate both the exponential factor due to the linear loss and the lumped amplification [49]; (b) Eq. (2) can be reduced to a higher-order NLS equation with $\alpha(z) = \alpha_1$, $\beta(z) = \alpha_2$, $\delta_1(z) = -\alpha_3$, $\delta_2(z) = -\alpha_4$, $\delta_3(z) = -\alpha_5$ and $\gamma(z) = \Gamma_1(z) = \Gamma_2(z) = 0$, which governs the femtosecond light pulses in an optical fiber, where α_1, α_2, α_3, α_4 and α_5 are all the real parameters with some soliton solutions for the higher-order NLS equation that have been constructed via a scaling transformation [50,51]; (c) when $\alpha(z) = 1/2$, $\beta(z) = 1, \delta_1(z) = \alpha_3, \delta_2(z) = \alpha_1, \delta_3(z) = \alpha_2 - \alpha_1$ and $\gamma(z) = \Gamma_1(z) = \Gamma_2(z) = 0$, Eq. (2) can be reduced to a extended third-order cubic NLS equation which describes the slow evolution of the wave envelope in nonlinear dispersive system, and soliton solutions have been derived based on the Galilean transformation and generalized Galilean invariance [52]; and (d) under the Hirota conditions $\alpha(z)\delta_2(z) = 3\beta(z)\delta_1(z)$ and $\delta_2(z) = -\delta_3(z)$, Eq. (2) can be reduced to a variable-coefficient Hirota equation [45–47], analytic multi-soliton solutions for which have been obtained via the bilinear method [46] and Darboux transformation [47], respectively.

Dromion structures have been investigated in the (2+1)- or higher- dimensional partial differential equations (PDEs) [53–58], which have hardly been obtained in the $(1 + 1)$-dimensional PDEs [59]. For instance, dromion solutions for the $(2 + 1)$- and $(3 + 1)$-dimensional Korteweg-de Vries equations have been reported [53,54], respectively. Dromion solutions for the Davey–Stewartson (DS) have been obtained explicitly [55] and numerically [56]. Dromion solutions for the noncommutative DS equations have been derived via the Darboux transformation [57]. Dromions for the $(2 + 1)$-dimensional NLS equation with nonlinearity coefficients have been constructed via the Hirota's bilinear method [58]. Dromion-like structures for the variable-coefficient Ginzburg–Landau equation have been studied [59]. Lump solitons, which is a kind of dromion-like solutions, for the KP and the generalized KP and BKP equations have been constructed [60]

However, to our knowledge, for Eq. (2), interactions between/among the subpicosecond or femtosecond solitons and dromion-like structures based on the analytic soliton solutions have not been discussed. In this paper, we will devote to obtain the soliton solutions and dromion-like structures via the Hirota's bilinear method and to discuss the interactions between/among the subpicosecond or femtosecond solitons. In Sect. 2, we will derive the variable-coefficient bilinear equations for Eq. (2) via symbolic computation. In Sect. 3, one-, two- and three-soliton solutions for Eq. (2) will be obtained, interactions between/among the two and three solitons will be discussed with different values of variable coefficients, and bound states and dromion-like structures will be presented. Our conclusions will be given in Sect. 4.

2 Bilinear equations and integrable constraints for Eq. (2)

With the dependent-variable transformation [45]

$$u(z,t) = A(z)g(z,t)/f(z,t), \tag{3}$$

Eq. (2) can be transformed into

$$\begin{aligned} & iA(z)\frac{D_z g\cdot f}{f^2} + iA(z)_z\frac{g}{f} + \alpha(z)A(z) \\ & \times\left(\frac{D_t^2 g\cdot f}{f^2} - \frac{g}{f}\frac{D_t^2 f\cdot f}{f^2}\right) + \beta(z)A(z)^3\frac{g^2 g^*}{f^3} \\ & + i\gamma(z)\frac{D_t g\cdot f}{f^2} + iA(z)\delta_1(z) \\ & \times\left(\frac{D_t^3 g\cdot f}{f^2} - 3\frac{D_t g\cdot f}{f^2}\frac{D_t^2 f\cdot f}{f^2}\right) \\ & + i\delta_2(z)A(z)^3\left(\frac{g^2 D_t g^*\cdot f}{f^4} + \frac{2gg^* D_t g\cdot f}{f^4}\right) \\ & + i\delta_3(z)A(z)^3\left(\frac{g^2 D_t g^*\cdot f + gg^* D_t g\cdot f}{f^4}\right) \\ & + A(z)\left[\Gamma_1(z) + i\Gamma_2(z)\right]g/f = 0, \end{aligned} \tag{4}$$

where $f(z,t)$ and $A(z)$ are the real functions, $g(z,t)$ is a complex one, the asterisk denotes the complex conjugate, D_z and D_t are the Hirota's bilinear derivative operators defined by [61]

$$\begin{aligned} & D_z^m D_t^n \Phi(z,t)\cdot\Psi(z,t) \equiv \left(\frac{\partial}{\partial z} - \frac{\partial}{\partial z'}\right)^m \\ & \times\left(\frac{\partial}{\partial t} - \frac{\partial}{\partial t'}\right)^n \Phi(z,t)\Psi(z',t')|_{z'=z,t'=t}, \end{aligned} \tag{5}$$

where z' and t' are the formal variables, $\Phi(z,t)$ and $\Psi(z,t)$ are the differentiable functions of z and t, m and n are the nonnegative integers. Assuming that $D_t^2 f\cdot f = \kappa gg^*$, where κ is a positive constant, we can transform Eq. (4) into

$$\begin{aligned} & \frac{A(z)\left[iD_z + \alpha(z)D_t^2 + i\gamma(z)D_t + i\delta_1(z)D_t^3 + \Gamma_1(z)\right]g\cdot f}{f^2} \\ & + \frac{ig[A(z)\Gamma_2(z) + A(z)_z]}{f} + \frac{A(z)g}{f^4}\left\{|g|^2 f\left[A(z)^2\beta(z)\right.\right. \\ & \left. - \kappa\alpha(z)\right] + iA(z)^2 g\left[\delta_2(z) + \delta_3(z)\right]D_t g^*\cdot f \\ & \left. + g^* D_t g\cdot f\left[3\kappa\delta_1(z) - A(z)^2(2\delta_1(z) + \delta_3(z))\right]\right\} = 0. \end{aligned} \tag{6}$$

Splitting Eq. (6) [45,62] yields

$$\begin{aligned} & \Big[iD_z + \alpha(z)D_t^2 + i\gamma(z)D_t + i\delta_1(z)D_t^3 + \Gamma_1(z) \\ & + iA(z)\Gamma_2(z) + iA(z)_z\Big]g\cdot f = 0, \end{aligned} \tag{7a}$$

$$A(z)^2\beta(z) - \kappa\alpha(z) = 0, \tag{7b}$$

$$\delta_2(z) + \delta_3(z) = 0, \tag{7c}$$

$$3\kappa\delta_1(z) - A(z)^2\left[2\delta_2(z) + \delta_3(z)\right] = 0. \tag{7d}$$

For Eq. 6, we can choose $iA(z)\Gamma_2(z) + iA(z)_z = 0$ which leads to $A(z) = e^{-\int \Gamma_2(z)\mathrm{d}z}$. From Eq. 7b–d, we get the constraints

$$\begin{aligned} & \beta(z) = \kappa\alpha(z)e^{2\int \Gamma_2(z)\mathrm{d}z},\ \delta_3(z) = -\delta_2(z), \\ & \delta_2(z) = 3\kappa\delta_1(z)e^{2\int \Gamma_2(z)\mathrm{d}z}, \end{aligned} \tag{8}$$

which are similar to the Hirota conditions [45–47]. Under Constraints (8), the variable-coefficient bilinear equations are derived as

$$\begin{aligned} & D_t^2 f\cdot f = \kappa gg^*, \\ & \left[iD_z + \alpha(z)D_t^2 + i\gamma(z)D_t + i\delta_1(z)D_t^3 + \Gamma_1(z)\right]g \\ & \cdot f = 0. \end{aligned} \tag{9}$$

3 Soliton solutions for Eq. (2) under Constraints (8)

In this part, we will derive the soliton solutions for Eq. (2) by expanding f and g as

$$\begin{aligned} & f = 1 + \epsilon f_1 + \epsilon^2 f_2 + \epsilon^3 f_3\cdots, \\ & g = g_0(1 + \epsilon g_1 + \epsilon^2 g_2 + \epsilon^3 g_3)\ldots, \end{aligned} \tag{10}$$

with ϵ as a formal expansion parameter, g_i's (i = 1,2,3...) are the complex functions of z and t, and f_k's (k =1,2,3...) are the real ones. The solutions can be constructed by substituting Expressions (10) into Bilinear Equation (9) and collecting terms proportional to the same powers of ϵ.

3.1 One-soliton solutions for Eq. (2) under Constraints (8)

Truncating Expressions (10) as

$$g = \epsilon g_1, \quad f = 1 + \epsilon^2 f_2, \tag{11}$$

substituting Expressions (11) into Bilinear Equations (9) and setting $\epsilon = 1$, we can obtain the one-soliton solutions for Eq. (2) under Constraints (8) as

$$u = A(z)\frac{g_1}{1 + f_2} \tag{12}$$

where

$$g_1 = e^{\eta}, \quad f_2 = Be^{\eta+\eta^*}, \quad B = \frac{\kappa}{2(k + k^*)^2},$$
$$\eta = kt + \int \left[ik^2\alpha(z) + i\Gamma_1(z) - k\gamma(z) - k^3\delta_1(z)\right] \mathrm{d}z + \phi$$

with k being a complex constant, and ϕ is a real one. Taking $k = k_R + k_I i$, where the subscripts R and I denote the real and imaginary parts, respectively, we obtain the intensity of the optical pulse as

$$|u|^2 = \mathrm{e}^{-2\int \Gamma_2(z)\mathrm{d}z}\frac{2k_R^2}{\kappa}\mathrm{sech}^2\left(\eta_R + \frac{1}{2}\ln\frac{\kappa}{8k_R^2}\right), \tag{13}$$

with

$$\eta_R = k_R t - k_R \int \Big[2k_I\alpha(z) + \gamma(z) + (k_R^2 - 3k_I^2)\delta_1(z)\Big]\mathrm{d}z. \tag{14}$$

To derive the velocity for a soliton, we can track a point of the soliton where the intensity keeps unchanged, from which a characteristic line equation can be written as

$$k_R t - k_R \int \Big[2k_I\alpha(z) + \gamma(z) + (k_R^2 - 3k_I^2)\delta_1(z)\Big]\mathrm{d}z + \frac{1}{2}\ln\frac{\kappa}{8k_R^2} = \text{constant}. \tag{15}$$

Differentiating Eq. (15) with respect to z, we obtain

$$\frac{\mathrm{d}t}{\mathrm{d}z} - \Big[(k_R^2 - 3k_I^2)\delta_1(z) + 2k_I\alpha(z) + \gamma(z)\Big] = 0, \tag{16}$$

from which we derive the velocity for the soliton as

$$v = \frac{\mathrm{d}z}{\mathrm{d}t} = \frac{1}{(k_R^2 - 3k_I^2)\delta_1(z) + 2k_I\alpha(z) + \gamma(z)}. \tag{17}$$

From the intensities of one-soliton solutions (12), we find that the soliton amplitude is related to the real part of the wave number, k, and that the velocity of the soliton is determined by the TOD $\delta_1(z)$, GVD $\alpha(z)$ and $\gamma_1(z)$ resulting from the group velocity. Linear gain/loss term, $\Gamma_2(z)$, can directly affect the soliton amplitude. Soliton width is related to the TOD, GVD, $\gamma_1(z)$ and wave number k. We present some figures with different values of the variable coefficients to illustrate those properties. In Fig. 1, we find that the variable coefficients, $\alpha(z)$, $\delta_1(z)$ and $\gamma(z)$, can

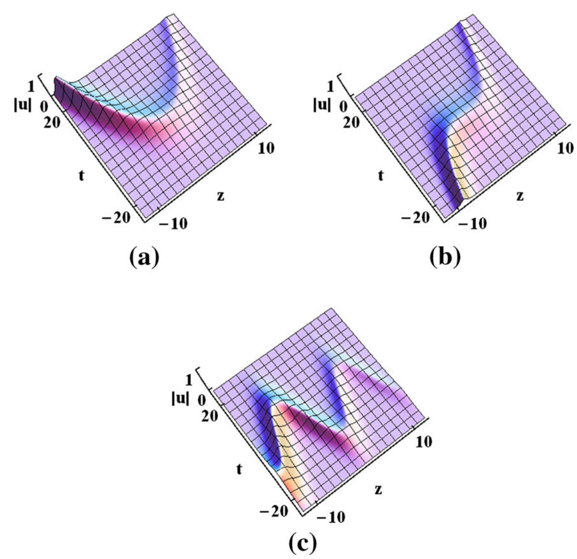

Fig. 1 One solitons via Solutions (12), with the parameters as $k = 1/4 + i/3$, $\kappa = 2$, $\Gamma_1(z) = z$, $\Gamma_2(z) = 1/10$, $\phi = 0$: **a** $\alpha(z) = z/2$, $\gamma(z) = z/4$, $\delta_1(z) = z/3$; **b** $\alpha(z) = z^2/10$, $\gamma(z) = z^2/20$, $\delta_1(z) = z^2/15$; **c** $\alpha(z) = 3\sin(z/2)$, $\gamma(z) = 3\sin(z/2)$, $\delta_1(z) = 3\cos(z/2)$

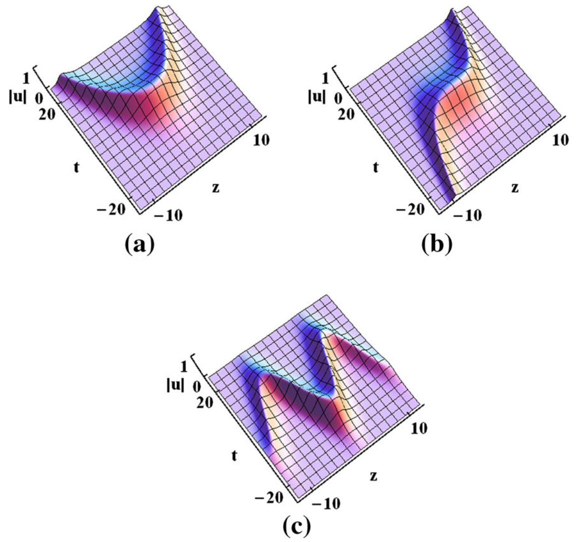

Fig. 2 The same as Fig. 1 except that $\Gamma_2(z) = z/50$

influence the structure, amplitude and velocity of the soliton: Velocity and amplitude change all the time along the z-axis; when $\alpha(z) = z/2$, $\delta_1(z) = z/3$ and $\gamma(z) = z/4$, we obtain a parabolic soliton via Solutions (12), as shown in Fig. 1a; when $\alpha(z) = z^2/10$, $\delta_1(z) = z^2/15$ and $\gamma(z) = z^2/20$, we plot a cubic soliton via Solutions (12), as seen in Fig. 1b. In Fig. 1c, when $\alpha(z) = 3\sin(z/2)$, $\delta_1(z) = 3\cos(z/2)$ and $\gamma(z) = 3\sin(z/2)$, we present a periodical oscillating soliton via Solutions (12). Further, influence of $\Gamma_2(z)$ can be seen when we compare Figs. (1) and (2): When $\Gamma_2(z) = 1/10$, we derive that $\mathrm{e}^{-2\int \Gamma_2(z)\mathrm{d}z} = \mathrm{e}^{-z/5}$ which leads to the soliton amplitude compressed along the z-axis, as seen in Fig. 1. As $\Gamma_2(z) = z/50$, we can derive that $\mathrm{e}^{-2\int \Gamma_2(z)\mathrm{d}z} = -\mathrm{e}^{z^2/50}$ which leads to the soliton amplitude compressed along the z-axis on both directions, as shown in Fig. 2.

3.2 Two-soliton solutions for Eq. (2) under Constraints (8)

In order to obtain the two-soliton solutions, we truncate Expressions (10) as

$$g = \epsilon g_1 + \epsilon^3 g_3, \quad f = 1 + \epsilon^2 f_2 + \epsilon^4 f_4. \tag{18}$$

Substituting Expressions (18) into Bilinear Equations (9) and setting $\epsilon = 1$, we obtain the two-soliton solutions for Eq. (2) under Constraints (8) as

$$u = A(z)\frac{g_1 + g_3}{1 + f_2 + f_4}, \tag{19}$$

where

$$\begin{aligned}
g_1 &= e^{\eta_1} + e^{\eta_2},\\
g_3 &= A_{123}e^{\eta_1+\eta_2+\eta_1^*} + A_{124}e^{\eta_1+\eta_2+\eta_2^*},\\
f_2 &= A_{13}e^{\eta_1+\eta_1^*} + A_{23}e^{\eta_2+\eta_1^*}\\
&\quad + A_{14}e^{\eta_1+\eta_2^*} + A_{24}e^{\eta_2+\eta_2^*},\\
f_4 &= A_{1234}e^{\eta_1+\eta_2+\eta_1^*+\eta_2^*}, \eta_m = k_m t\\
&\quad + w_m(z) + \phi_m,\\
w_m(z) &= \int \left[i k_m^2 \alpha(z) - k_m \gamma(z) - k_m^3 \delta_1(z) \right] \mathrm{d}z,\\
A_{m,n+2} &= \kappa/2(k_m + k_n^*)^2, \quad (m = 1, 2), \quad (n = 1, 2),\\
A_{12} &= 2(k_1 - k_2)^2/\kappa, \quad A_{34} = 2(k_1^* - k_2^*)^2/\kappa,\\
A_{123} &= A_{12}A_{13}A_{23}, A_{124} = A_{12}A_{14}A_{24},\\
A_{1234} &= A_{123}A_{14}A_{24}A_{34},
\end{aligned}$$

with k_1 and k_2 being the complex constants, and ϕ_m's as the real ones. Via symbolic computation and Solutions (19), intensity of the two-soliton solutions can be written as

$$|u|^2 = \mathrm{e}^{\int[-2\Gamma_2(z)]\mathrm{d}z} \frac{|\xi_1|^2 + |\xi_2|^2 + 2\chi}{[C_0 + 2re^{\eta_{1R}+\eta_{2R}}\cos(\eta_{1I} - \eta_{2I} + \varphi)]^2}, \tag{20}$$

where

$$\begin{aligned}
C_0 &= 1 + A_{13}e^{\eta_1+\eta_1^*} + A_{24}e^{\eta_2+\eta_2^*}\\
&\quad + A_{1234}e^{\eta_1+\eta_2+\eta_1^*+\eta_2^*},\\
A_{123} &= r_1 e^{i\varphi_1}, A_{124} = r_2 e^{i\varphi_2}, A_{14} = re^{i\varphi},\\
k_1 &= a_1 + b_1 i, \xi_1 = e^{\eta_{1R}} + r_2 e^{2\eta_{2R}+\eta_{1R}+i\varphi_2},\\
k_2 &= a_2 + b_2 i, \xi_2 = e^{\eta_{2R}} + r_1 e^{2\eta_{1R}+\eta_{2R}+i\varphi_1},\\
\chi &= 2r_1 e^{3\eta_{1R}+\eta_{2R}}\cos(\eta_{2I} - \eta_{1I} + \varphi_1)\\
&\quad + 2r_2 e^{\eta_{1R}+3\eta_{2R}}\cos(\eta_{2I} - \eta_{1I} - \varphi_2)\\
&\quad + 2e^{\eta_{1R}+\eta_{2R}}\cos(\eta_{2I} - \eta_{1I})\\
&\quad + 2r_1r_2 e^{3\eta_{1R}+3\eta_{2R}}\cos(\eta_{2I} - \eta_{1I} + \varphi_1 - \varphi_2),\\
\eta_{1I} &= b_1 t - \int \Big[(b_1^2 - a_1^2)\alpha(z) + b_1\gamma(z)\\
&\quad + (3a_1^2 - b_1^2)b_1\delta_1(z) - \Gamma_1(z) \Big] \mathrm{d}z,\\
\eta_{2I} &= b_2 t - \int \Big[(b_2^2 - a_2^2)\alpha(z) + b_2\gamma(z)\\
&\quad + (3a_2^2 - b_2^2)b_2\delta_1(z) - \Gamma_1(z) \Big] \mathrm{d}z,
\end{aligned} \tag{21}$$

it is obvious that periods exist in the two-soliton solutions.

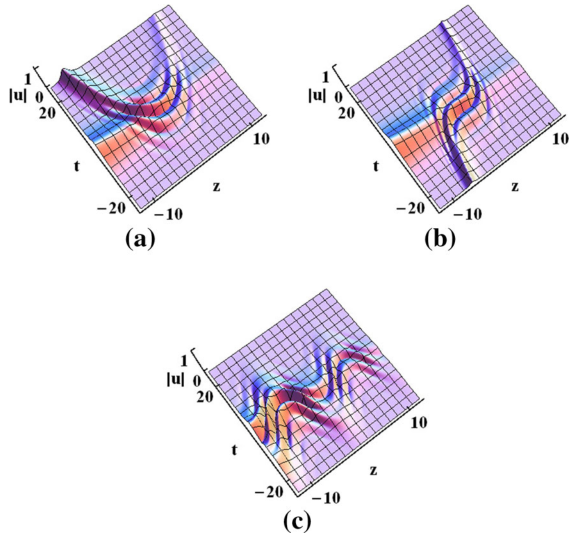

Fig. 3 Interactions between the two solitons via Solutions (19), with the parameters as $k_1 = 1/3 + (1 + \sqrt{13/3})i/3$, $k_2 = 1/4 + i/5$, $\kappa = 4$, $\Gamma_1(z) = z$, $\Gamma_2(z) = 1/10$, $\phi_1 = \phi_2 = 0$: **a** $\alpha(z) = \gamma(z) = \delta_1(z) = z/2$; **b** $\alpha(z) = \gamma(z) = \delta_1(z) = z^2/5$; **c** $\alpha(z) = \gamma(z) = \delta_1(z) = 3\sin(z/2)$

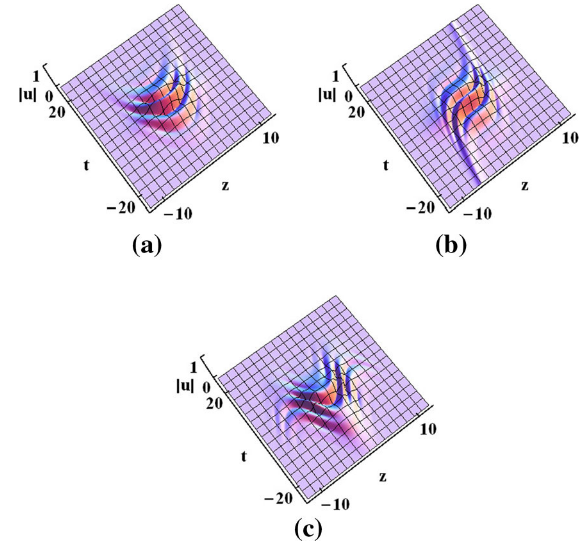

Fig. 4 The same as Fig. 3 except that $\Gamma_2(z) = z/10$, $\kappa = 2$

Interactions between the two solitons are presented in Figs. 3 and 4: When $\alpha(z) = \delta_1(z) = \gamma(z) = z/2$, interaction between a parabolic and static soliton can be seen in Fig. 3a, where the intensity approaches to zero quickly along the z-axis; When $\alpha(z) = \delta_1(z) = \gamma(z) = z^2/5$, interaction between the cubic and static solitons is obtained in Fig. 3b; when $\alpha(z) = \delta_1(z) = \gamma(z) = 3\sin(z/2)$, interaction between the periodic and static solitons is presented in Fig. 3c. Although the intensities of the two solitons in Fig. 3 decay exponentially along the z-axis, attenuation degree of which in Fig. 3c is much weaker than that in Fig. 3a, b. Compared with Fig. 3, if we take $\Gamma_2(z) = z/10$, interaction features between the two solitons in this case are similar to those in Fig. 3 except that the intensities decrease along the z- axis in both directions, as presented in Fig. 4.

Bound-state solitons can be obtained with certain parameters: For a bound-state soliton, we choose two static solitons to satisfy the limitation that the two solitons have the same velocity and to derive an explicit relation between a and b from Eq. (17) as $b = (\alpha(z) \pm \sqrt{\alpha(z)^2 + 3\delta_1(z)\gamma(z) + 3a^2\delta_1(z)^2})/(3\delta_1(z))$. Because b is a constant in the soliton solution, we need to introduce a set of the constraints among the variable coefficients as $\alpha(z) = c_1\gamma(z) = c_2\delta_1(z)$, with c_1 and c_2 being two real constants. For the sake of brevity, we can take $\alpha(z) = \gamma(z) = \delta_1(z)$, i.e., $c_1 = c_2 = 1$, the relation between a and b can be rewritten as $b = (1 \pm \sqrt{4 + 3a^2})/3$. For the two solitons propagating with the same velocity, we have $b_\rho = (1 \pm \sqrt{4 + 3\rho^2})/3$, $(\rho = 1, 2)$ so as to derive that $\eta_{2I} - \eta_{1I} = (b_2 - b_1)t + \Gamma \int \alpha(z)\mathrm{d}z$, where $\Gamma = 8\left(\sqrt{4 + 3a_1^2} + 3a_1^2\sqrt{4 + 3a_1^2} - \sqrt{4 + 3a_2^2} - 3a_2^2\sqrt{4 + 3a_2^2}\right)$.

Studies on the bound-state solitons can be carried out for different variable coefficients: (a) Setting $\Gamma \int \alpha(z)\mathrm{d}z = 2n\pi$ and $\alpha(z) = \zeta z$, with ζ being a real constant, we can obtain $|\Gamma|\zeta z_n^2/2 = 2n\pi$ $(n = 1, 2, 3 \ldots)$, which leads to $z_n = 2\sqrt{n}\sqrt{\pi/|\Gamma|\zeta}$, from which the quasiperiodic formulae along the z-axis can be expressed as $T_n = 2(\sqrt{n} - \sqrt{n-1})\sqrt{\pi/|\Gamma|\zeta}$. In this case, when we choose the variable coefficients as $\alpha(z) = \gamma(z) = \delta_1(z) = 2z$, the two-soliton solutions evolve into a quasiperiodic bound state, as shown in Fig. 5a. Quasiperiodic attractions and repulsions lead to the redistribution of the energy between the two solitons. Furthermore, we can calculate the quasi-periods of the bound state. Using the parameters given in Fig. 5a, we obtain the periods $T_1 = 7.834$, $T_2 = 3.245$ and $T_3 = 2.450$. Meanwhile, we can derive the ratio among the quasi-periods, which is $T_1 : T_2 : T_3 \cdots = 1 : (\sqrt{2} - 1) : (\sqrt{3} - \sqrt{2}) \cdots$;

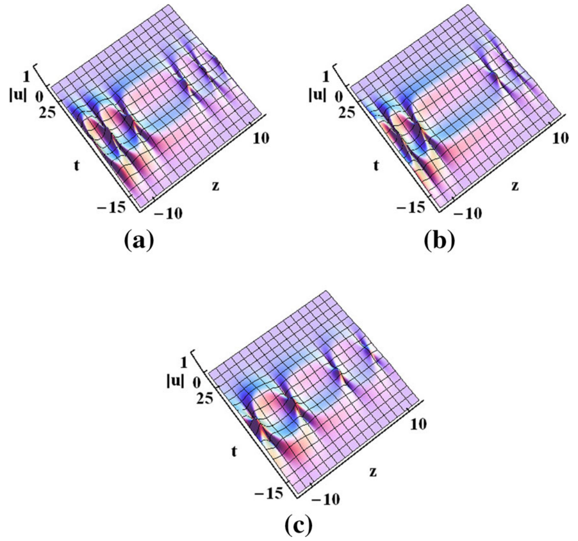

Fig. 5 Bound states via Solutions (19), with the parameters as $k_1 = 1/3 + (1 + \sqrt{13/3})i/3$, $k_2 = 1/4 + (1 + \sqrt{67}/4)i/3$, $\kappa = 2$, $\Gamma_1(z) = z$, $\Gamma_2(z) = 1/12$, $\phi_1 = \phi_2 = 0$: **a** $\alpha(z) = \gamma(z) = \delta_1(z) = 2z$; **b** $\alpha(z) = \gamma(z) = \delta_1(z) = z^2/5$; **c** $\alpha(z) = \gamma(z) = \delta_1(z) = 10\sin(z/5)$

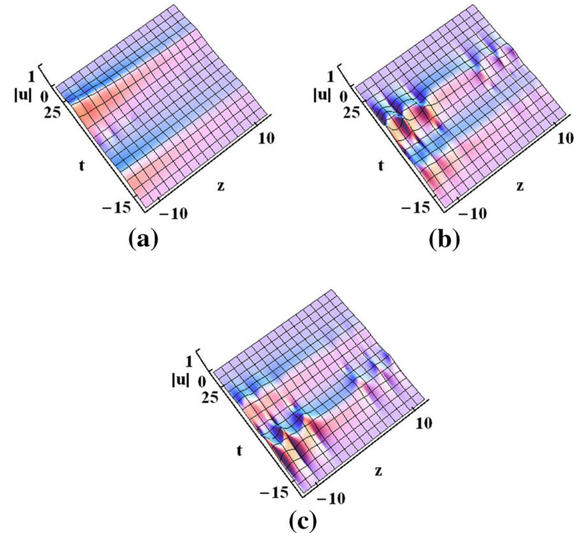

Fig. 6 The same as Fig. 5a except that **a** $\phi_1 = -5/2$, $\phi_2 = 5/2$; **b** $\phi_1 = -1/2$, $\phi_2 = 1/2$; **c** $\phi_1 = 1/2$, $\phi_2 = -1/2$

(b) if $\alpha(z) = \zeta z^2$, with ζ being a real constant, we can obtain $|\Gamma|\zeta z_n^3/3 = 2n\pi$ $(n = 1, 2, 3 \ldots)$, which leads to $z_n = \sqrt[3]{n}\sqrt[3]{6\pi/|(\Gamma|\zeta)}$, from which the quasiperiodic formulae along the z-axis can be expressed as $T_n = (\sqrt[3]{n} - \sqrt[3]{n-1})\sqrt[3]{6\pi/|(\Gamma|\zeta)}$. As shown in Fig. 5b, where $\alpha(z) = \gamma(z) = \delta_1(z) = z^2/5$, we present a bound state which is similar to that in Fig. 5a. Using the parameters given in Fig. 5, we derive the periods of the bound state ($T_1 = 9.728$, $T_2 = 2.528$ and $T_3 = 1.774$); and (c) setting $\alpha(z) = \zeta\cos(\varpi z)$, where ζ and ϖ are both the real constants, we obtain $|\Gamma|\zeta\sin(\varpi z_n)/\varpi = 2n\pi(n = 1, 2, 3 \ldots)$. Due to the fact that $\cos(\varpi z)$ is a periodic function, $2\pi/\varpi$ is one of the periods. In addition, the quasiperiodic formulae can be expressed as $T_n = \arcsin(2\pi\varpi\frac{n}{\Gamma\zeta})/\varpi - \arcsin(2\pi\varpi\frac{n-1}{\Gamma\zeta})/\varpi$. With the parameters given in Fig. 5c, the periods can also be derived.

As shown in Fig. 6a, when $\phi_1 = -5/2$ and $\phi_2 = 5/2$ which are related to the initial position, we plot two static solitons which are parallel to the z-axis. The two solitons propagate along the z-axis in the optical fiber with a constant separation between them. After we set $\phi_1 = -1/2$ and $\phi_2 = 1/2$, an interaction between the two parallel solitons is obtained, as seen in Fig. 6b. When we change the parameters to $\phi_1 = 0$ and $\phi_2 = 0$, the bound is achieved, as depicted in Fig. 5a. When $\phi_1 = 1/2$ and $\phi_2 = -1/2$, an interaction similar to that in Fig. 6b between the two solitons is presented, as seen in Fig. 6c. From the above, we find that the parameters ϕ_1 and ϕ_2 related to the initial positions can influence the separation and interaction between the two solitons.

3.3 Three-soliton solutions for Eq. (2) under Constraints (8)

To derive the three-soliton solutions for Eq. (2) under Constraints (8), we truncate Expressions (10) as

$$g = \epsilon g_1 + \epsilon^3 g_3 + \epsilon^5 g_5,$$
$$f = 1 + \epsilon^2 f_2 + \epsilon^4 f_4 + \epsilon^6 f_6, \tag{22}$$

substituting Eq. (22) into Bilinear Equations (9) and setting $\epsilon = 1$, we can derive the three-soliton solutions for Eq. (2) as

$$u = \frac{g_1 + g_3 + g_5}{1 + f_2 + f_4 + f_6}, \tag{23}$$

where

$$g_1 = e^{\eta_1} + e^{\eta_2} + e^{\eta_3},\ g_3 = A_{124}e^{\eta_1+\eta_2+\eta_1^*} + A_{125}e^{\eta_1+\eta_2+\eta_2^*} + A_{126}e^{\eta_1+\eta_2+\eta_3^*} + A_{134}e^{\eta_1+\eta_3+\eta_1^*} + A_{135}e^{\eta_1+\eta_3+\eta_2^*} + A_{136}e^{\eta_1+\eta_3+\eta_3^*} + A_{234}e^{\eta_2+\eta_3+\eta_1^*} + A_{235}e^{\eta_2+\eta_3+\eta_2^*} + A_{236}e^{\eta_2+\eta_3+\eta_3^*},$$

$$g_5 = A_{12345}e^{\eta_1+\eta_2+\eta_3+\eta_1^*+\eta_2^*} + A_{12346}e^{\eta_1+\eta_2+\eta_3+\eta_1^*+\eta_3^*} + A_{12356}e^{\eta_1+\eta_2+\eta_3+\eta_2^*+\eta_3^*},$$

$$f_2 = A_{14}e^{\eta_1+\eta_1^*} + A_{24}e^{\eta_2+\eta_1^*} + A_{34}e^{\eta_3+\eta_1^*} + A_{15}e^{\eta_1+\eta_2^*} + A_{25}e^{\eta_2+\eta_2^*} + A_{35}e^{\eta_3+\eta_2^*} + A_{16}e^{\eta_1+\eta_3^*} + A_{26}e^{\eta_2+\eta_3^*} + A_{36}e^{\eta_3+\eta_3^*},$$

$$f_4 = A_{1245}e^{\eta_1+\eta_2+\eta_1^*+\eta_2^*} + A_{1246}e^{\eta_1+\eta_2+\eta_1^*+\eta_3^*} + A_{1256}e^{\eta_1+\eta_2+\eta_2^*+\eta_3^*} + A_{1345}e^{\eta_1+\eta_3+\eta_1^*+\eta_2^*} + A_{1346}e^{\eta_1+\eta_3+\eta_1^*+\eta_3^*} + A_{1356}e^{\eta_1+\eta_3+\eta_2^*+\eta_3^*} + A_{2345}e^{\eta_2+\eta_3+\eta_1^*+\eta_2^*} + A_{2346}e^{\eta_2+\eta_3+\eta_2^*+\eta_3^*} + A_{2356}e^{\eta_2+\eta_3+\eta_2^*+\eta_3^*},$$

$$f_6 = A_{123456}e^{\eta_1+\eta_2+\eta_3+\eta_1^*+\eta_2^*+\eta_3^*},$$

$$\eta_p = k_p t + w_p(z) + \phi_p,$$

$$w_p(z) = \int \left[i\alpha(z)k_p^2 - \gamma(z)k_p - \delta_1(z)k_p^3\right] dz,$$

$$A_{p,q+3} = \frac{\kappa}{2(k_p + k_q^*)^2},\ (p = 1, 2, 3),\ (q = 1, 2, 3),$$

$$A_{12} = \frac{2(k_1 - k_2)^2}{\kappa}, A_{13} = \frac{2(k_1 - k_3)^2}{\kappa},$$

$$A_{23} = \frac{2(k_2 - k_3)^2}{\kappa}, A_{45} = \frac{2(k_1^* - k_2^*)^2}{\kappa},$$

$$A_{46} = \frac{2(k_1^* - k_3^*)^2}{\kappa}, A_{56} = \frac{2(k_2^* - k_3^*)^2}{\kappa},$$

$$A_{m_1m_2m_3} = A_{m_1m_2}A_{m_2m_3}A_{m_1m_3}, (m_1 \neq m_2 \neq m_3),$$

$$A_{n_1n_2n_3n_4} = A_{n_1n_2}A_{n_1n_3}A_{n_1n_4}A_{n_2n_3}A_{n_2n_4}A_{n_3n_4}, (n_1 \neq n_2 \neq n_3 \neq n_4),$$

$$A_{12345} = A_{123}A_{145}A_{24}A_{25}A_{34}A_{35},$$
$$A_{12346} = A_{123}A_{146}A_{24}A_{26}A_{34}A_{36},$$
$$A_{12356} = A_{123}A_{156}A_{25}A_{26}A_{35}A_{36},$$
$$A_{123456} = A_{123}A_{145}A_{246}A_{356}A_{16}A_{25}A_{34},$$

with r_1, r_2 and r_3 being the complex constants.

Figure 7 presents the interactions among the three solitons for Eq. (2). As seen in Fig. 7a, b, separations among them decrease along the optical fiber. The gain/loss term, $\gamma_2(z)$, leads to the exponential decay for the intensity of solitons. Three parallel solitons propagate along the z-axis periodically, as shown in Fig. 7c, which is similar to that in Fig. 6a. As the three solitons are the representative example of the multi-solitons, discussing some interactions among them might be used for the future development of the optical fiber, and we consider the interaction between the bound state and a single soliton: As presented in Fig. 8a, we plot the interaction between the bound state and a parabolic soliton, from which we note that the interaction does not affect the structure and velocity of any of them except for a constant phase shift in the interaction area. In Fig. 8b, we can see the cubic soliton passes through the bound state and propagates along the z- axis and a constant phase shift is formed as well. Interaction between the bound state and a periodical oscillating soliton is plotted in Fig. 8c.

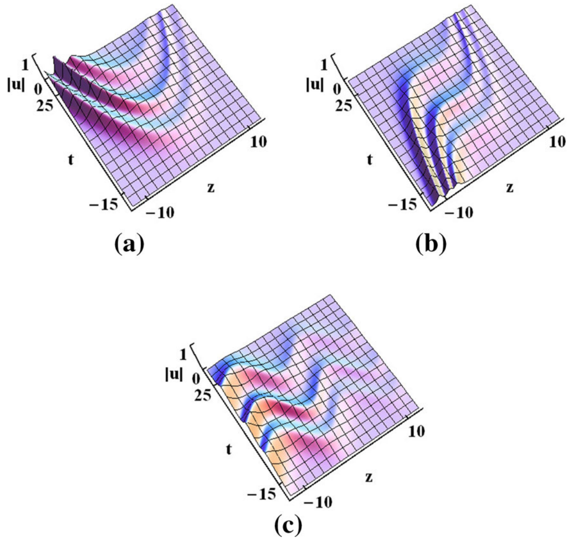

Fig. 7 Interactions among the three solitons via Solutions (23), with the parameters as $k_1 = 1/2 + i/3$, $k_2 = 1/3 + i/4$, $k_3 = 1/4 + i/5$, $\kappa = 8$, $\phi_1 = \phi_2 = 0$, $\Gamma_1(z) = z$, $\Gamma_2(z) = 1/8$: **a** $\alpha(z) = z/2$, $\gamma(z) = z/4$, $\delta_1(z) = z/3$; **b** $\alpha(z) = z^2/10$, $\gamma(z) = z^2/20$, $\delta_1(z) = z^2/15$; **c** $\alpha(z) = 2\sin(z/2)$, $\gamma(z) = 2\cos(z/2)$, $\delta_1(z) = 2\sin(z/2)$

3.4 Dromion-like structures for Eq. (2) under Constraints (8)

As shown in Fig. 9, we present the single dromion-like structures with different values of variable coefficients for Eq. (2) under Constraints (8) and find that the variable coefficients related to Eq. (2) can influence the dromion-like structures. For the two-soliton solutions, we present the double dromion-like structures, as presented in Fig. 10: In Fig. 10a, the double dromion-like structures do not interact, from which we find that the

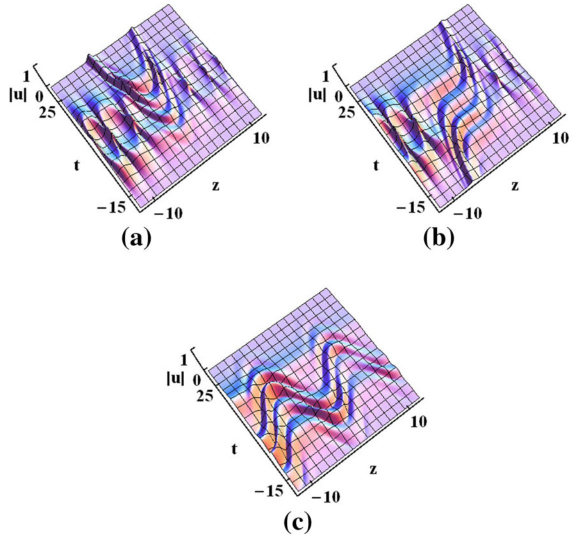

Fig. 8 Interactions between the bound state and a single soliton via Solutions (23), with the parameters as $k_1 = 1/3 + (1 + \sqrt{13/3})i/3$, $k_2 = 1/4 + (1 + \sqrt{67}/4)i/3$, $k_3 = 1/4 + i/3$, $\kappa = 4$, $\phi_1 = \phi_2 = \phi_3 = 0$, $\Gamma_1(z) = z$, $\Gamma_2(z) = 1/12$: **a** $\alpha(z) = \gamma(z) = \delta_1(z) = 2z$; **b** $\alpha(z) = \gamma(z) = \delta_1(z) = z^2/5$; **c** $\alpha(z) = \gamma(z) = \delta_1(z) = 3\sin(z/3)$

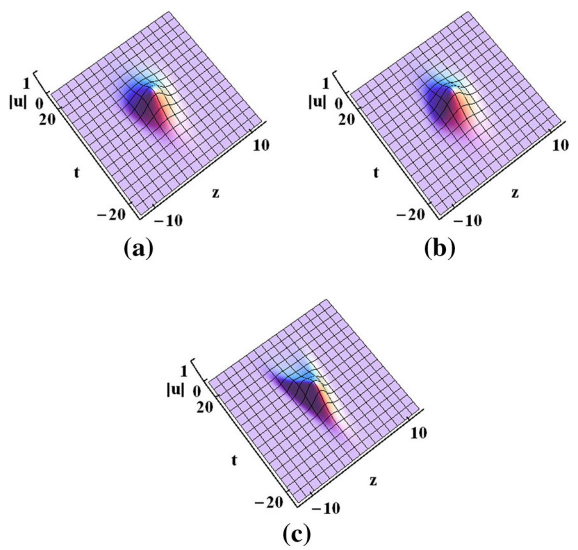

Fig. 9 Single dromion-like structures via Solutions (12), with the parameters as $k = 1/4 + i/3$, $\kappa = 1/5$, $\Gamma_1(z) = z$, $\Gamma_2(z) = z/3$, $\phi = 0$: **a** $\alpha(z) = z/2$, $\gamma(z) = z/4$, $\delta_1(z) = z/3$; **b** $\alpha(z) = z^2/10$, $\gamma(z) = z^2/20$, $\delta_1(z) = z^2/15$; **c** $\alpha(z) = 3\sin(z/2)$, $\gamma(z) = 3\sin(z/2)$, $\delta_1(z) = 3\cos(z/2)$

distance between them can be influenced by the parameters related to the initial positions. Seen in Fig. 10b is the double dromion-like structure which evolves from

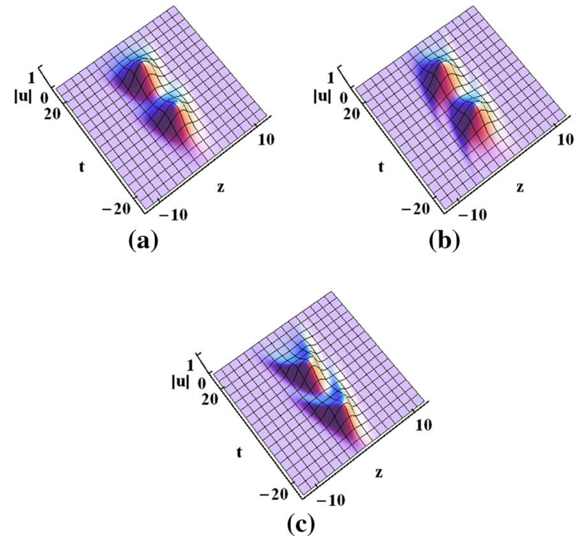

Fig. 10 Double dromion-like structures via Solutions (12), with the parameters as $k_1 = 1/3 + i/4$, $k_2 = 1/4 + i/5$, $\kappa = 1/5$, $\Gamma_1(z) = z$, $\Gamma_2(z) = z/3$, $\phi_1 = \phi_2 = 2$: **a** $\alpha(z) = \gamma(z) = \delta_1(z) = z/2$; **b** $\alpha(z) = \gamma(z) = \delta_1(z) = z^2/5$; **c** $\alpha(z) = \gamma(z) = \delta_1(z) = 3\sin(z/2)$

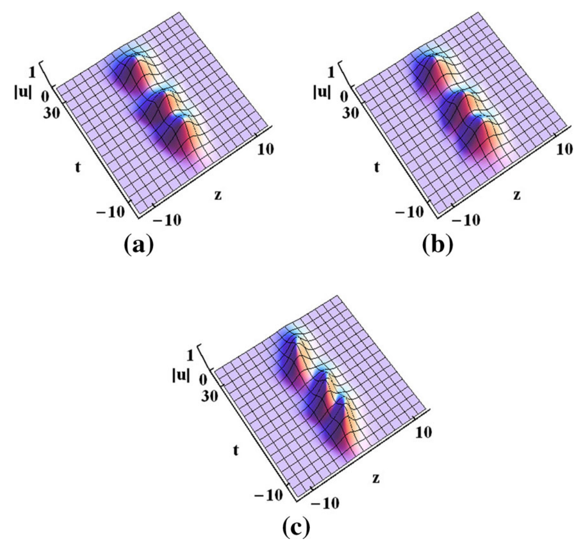

Fig. 11 Triple dromion-like structures via Solutions (23), with the parameters as $k_1 = 1/2 + i/3$, $k_2 = 1/3 + i/4$, $k_3 = 1/4 + i/5$, $\kappa = 1/3$, $\phi_1 = \phi_2 = \phi_3 = 0$, $\Gamma_1(z) = z$, $\Gamma_2(z) = z/3$: **a** $\alpha(z) = z/2$, $\gamma(z) = z/4$, $\delta_1(z) = z/3$; **b** $\alpha(z) = z^2/10$, $\gamma(z) = z^2/20$, $\delta_1(z) = z^2/15$; **c** $\alpha(z) = 2\sin(z/2)$, $\gamma(z) = 2\cos(z/2)$, $\delta_1(z) = 2\sin(z/2)$

the two cubic solitons. The double dromion-like structure in Fig. 10c is from the two periodically oscillating solitons, the distortion degree of which is much more serious than that in Fig. 10a, b. Triple dromion-like structures are shown in Fig. 11: There are three lumps in all of the figures, and the maximum values of the optical solitons are the same. The distortion of the figures is determined by the variable coefficients $\alpha(t)$ and $\gamma_1(t)$.

4 Conclusions

In this paper, with symbolic computation and modified Hirota method, Eq. (2), a higher-order variable-coefficient NLS equation for the propagation of subpicosecond and femtosecond pulses in an inhomogeneous optical fiber, has been investigated. Under integrable Constraints (8), Bilinear Equations (9) have been derived and one-, two- and three-soliton solutions have been obtained, i.e., Solutions (12), (19) and (23). Soliton amplitude has been found to be related to the real part of the wave number, k_R. Velocity of the soliton has been seen to be determined by the TOD $\delta_1(z)$, GVD $\alpha(z)$ and the group-velocity-related $\gamma_1(z)$. Linear gain/loss term, $\Gamma_2(z)$, has been found to lead to the soliton amplitude exponential decay along the z-axis. Soliton width has been seen to be determined by the TOD, GVD, $\gamma_1(z)$ and wave number k_R. Other results of the paper are summarized as follows:

1. The one-, two- and three-soliton solutions for Eq. (2) under Constraints (8) with different values of $\alpha(z)$, $\delta_1(z)$, $\gamma_1(z)$ and $\Gamma_2(z)$ have been discussed graphically: As seen in Figs. 1 and 2, we have presented the parabolic, cubic and periodically oscillating solitons with different values of $\alpha(z)$, $\gamma_1(z)$ and $\Gamma_2(z)$. In Figs. 3 and 4, interactions between the two solitons have been obtained.
2. For the two- and three-soliton solutions, we have presented the interactions and bound states with different values of $\alpha(z)$, $\delta_1(z)$, $\gamma_1(z)$ and $\Gamma_2(z)$: In Fig. 5, we have discussed the bound state evolving from the two solitons with certain parameters, and periods or quasi-periods have been calculated for each case, respectively. Separations and interactions between the two solitons influenced by the parameters ϕ_1 and ϕ_2 which are related to the initial positions have been analyzed, as seen in Fig. 6. Interactions among the three solitons have been shown in Fig. 7. Interactions between the bound state and a single soliton have been obtained in Fig. 8.
3. Dromion-like structures for Eq. (2) have been depicted in Figs. 9, 10 and 11: In Fig. 9, single dromion-like structures with different values of $\alpha(z)$, $\delta_1(z)$ and $\gamma_1(z)$ have been plotted. In Fig. 10, double dromion-like structures have been presented. Triple dromion-like structures have been addressed in Fig. 11: There are three lumps in all of the figures with different values of $\alpha(z)$, $\delta_1(z)$, $\gamma_1(z)$ and $\Gamma_2(z)$, and the distortions of the three solitons have been found to be determined by variable coefficients.

Acknowledgements We express our sincere thanks to the editors, reviewers and members of our discussion group for their valuable suggestions. This work has been supported by the National Natural Science Foundation of China under Grant No. 11272023 and by the Fund of State Key Laboratory of Information Photonics and Optical Communications (Beijing University of Posts and Telecommunications).

References

1. Wazwaz, A.M.: Gaussian solitary wave solutions for nonlinear evolution equations with logarithmic nonlinearities. Nonlinear Dyn. **83**, 591–596 (2016)
2. Wazwaz, A.M., El-Tantawy, S.A.: A new integrable (3+1)-dimensional KdV-like model with its multiple-soliton solutions. Nonlinear Dyn. **83**, 1529–1534 (2016)
3. Wazwaz, A.M., El-Tantawy, S.A.: A new (3+1)-dimensional generalized Kadomtsev–Petviashvili equation. Nonlinear Dyn. **84**, 1107–1112 (2016)
4. Zuo, D.W., Gao, Y.T., Meng, G.Q., Shen, Y.J., Yu, X.: Multi-soliton solutions for the three-coupled KdV equations engendered by the Neumann system. Nonlinear Dyn. **75**(4), 701–708 (2014)
5. Liu, D.Y., Tian, B., Jiang, Y., Sun, W.R.: Soliton solutions and Bäcklund transformations of a (2+1)-dimensional nonlinear evolution equation via the Jaulent–Miodek hierarchy. Nonlinear Dyn. **78**, 2341–2347 (2014)
6. Mirzazadeh, M.: Soliton solutions of Davey–Stewartson equation by trial equation method and ansatz approach. Nonlinear Dyn. **82**, 1775–1780 (2015)
7. Sun, Y.H., Gao, Y.T., Meng, G.Q., Yu, X., Shen, Y.J., Sun, Z.Y.: Bilinear forms and soliton interactions for two generalized KdV equations for nonlinear waves. Nonlinear Dyn. **78**, 349–357 (2014)
8. Sun, Z.Y., Gao, Y.T., Liu, Y., Yu, X.: Soliton management for a variable-coefficient modified Korteweg-de Vries equation. Phys. Rev. E **84**, 026606 (2011)
9. Saha, A., Chatterjee, P.: Solitonic, periodic, quasiperiodic and chaotic structures of dust ion acoustic waves in nonextensive dusty plasmas. Eur. Phys. J. D **69**, 1–8 (2015)
10. Zhen, H.L., Tian, B., Wang, Y.F., Liu, D.Y.: Soliton solutions and chaotic motions of the Zakharov equations for the Langmuir wave in the plasma. Phys. Plasmas **22**, 032307 (2015)
11. Zhen, H.L., Tian, B., Sun, Y., Chai, J., Wen, X.Y.: Solitons and chaos of the Klein-Gordon-Zakharov system in a high-frequency plasma. Phys. Plasmas **22**, 102304 (2015)

12. Zhang, J.: Stability of attractive Bose–Einstein condensates. J. Stat. Phys. **101**, 731–746 (2000)
13. Sun, W.R., Tian, B., Jiang, Y., Zhen, H.L.: Rogue matter waves in a Bose–Einstein condensate with the external potential. Eur. Phys. J. D **68**, 1–7 (2014)
14. Alakhaly, G.A., Dey, B.: Discrete breather and soliton-mode collective excitations in Bose–Einstein condensates in a deep optical lattice with tunable three-body interactions. Eur. Phys. J. D **69**, 1–7 (2015)
15. Andreev, P.A., Kuzmenkov, L.S.: Exact analytical soliton solutions in dipolar Bose–Einstein condensates. Eur. Phys. J. D **68**, 1–14 (2014)
16. Sun, W.R., Tian, B., Wang, Y.F., Zhen, H.L.: Soliton excitations and interactions for the three-coupled fourth-order nonlinear Schrödinger equations in the alpha helical proteins. Eur. Phys. J. D **69**, 1–9 (2015)
17. Jiang, H.J., Xiang, J.J., Dai, C.Q., Wang, Y.Y.: Nonautonomous bright soliton solutions on continuous wave and cnoidal wave backgrounds in blood vessels. Nonlinear Dyn. **75**, 201–207 (2014)
18. Agrawal, G.P.: Nonlinear Fiber Optics. Academic press, California (2007)
19. Sun, W.R., Tian, B., Jiang, Y., Zhen, H.L.: Optical rogue waves associated with the negative coherent coupling in an isotropic medium. Phys. Rev. E **91**(2), 023205 (2015)
20. Wang, H., Ling, D., Chen, G., Zhu, X., He, Y.: Defect solitons in nonlinear optical lattices with parity-time symmetric Bessel potentials. Eur. Phys. J. D **69**, 1–6 (2015)
21. Zhou, Q.: Soliton and soliton-like solutions to the modified Zakharov–Kuznetsov equation in nonlinear transmission line. Nonlinear Dyn. **83**, 1429–1435 (2016)
22. Hirota, R., Ohta, Y.: Hierarchies of coupled soliton equations. I. J. Phys. Soc. Jpn. **60**(3), 798–809 (1991)
23. Hirota, R.: Exact solution of the Korteweg-de Vries equation for multiple collisions of solitons. Phys. Rev. Lett. **27**(18), 1192 (1971)
24. Wazwaz, A.M.: Multiple kink solutions for two coupled integrable (2+1)-dimensional systems. Appl. Math. Lett. **58**, 1–6 (2016)
25. Wazwaz, A.M.: New (3+1)-dimensional nonlinear evolution equations with mKdV equation constituting its main part: multiple soliton solutions. Chaos Solitons Fractals **76**, 93–97 (2015)
26. Wazwaz, A.M.: Multiple soliton solutions for an integrable couplings of the Boussinesq equation. Ocean Eng. **73**, 38–40 (2013)
27. Mirzazadeh, M., Eslami, M., Zerrad, E., Mahmood, M.F., Biswas, A., Belic, M.: Optical solitons in nonlinear directional couplers by sine-cosine function method and Bernoullis equation approach. Nonlinear Dyn. **81**(4), 1933–1949 (2015)
28. Biswas, A., Mirzazadeh, M., Savescu, M., Milovic, D., Khan, K.R., Mahmood, M.F., Belic, M.: Singular solitons in optical metamaterials by ansatz method and simplest equation approach. J. Mod. Opt. **61**(19), 1550–1555 (2014)
29. Zhou, Q., Zhong, Y., Mirzazadeh, M., Bhrawy, A.H., Zerrad, E., Biswas, A.: Thirring combo-solitons with cubic nonlinearity and spatio-temporal dispersion. Waves Random Complex Media **26**(2), 204–210 (2016)
30. Wazwaz, A.M.: Variants of a (3+ 1)-dimensional generalized BKP equation: multiple-front waves solutions. Comput. Fluids **97**, 164–167 (2014)
31. Ma, W.X., Zhu, Z.: Solving the (3+ 1)-dimensional generalized KP and BKP equations by the multiple exp-function algorithm. Appl. Math. Comput. **218**(24), 11871–11879 (2012)
32. Ma, W.X.: Bilinear equations, Bell polynomials and linear superposition principle. J. Phys. Conf. Ser. **411**, 012021 (2013)
33. Ma, W.X.: A refined invariant subspace method and applications to evolution equations. Sci. China Math. **55**, 1769–1778 (2012)
34. Ma, W.X.: Generalized bilinear differential equations. Stud. Nonlinear Sci. **2**, 140–144 (2011)
35. Nakatsuka, H., Grischkowsky, D., Balant, A.C.: Nonlinear picosecond-pulse propagation through optical fibers with positive group velocity dispersion. Phys. Rev. Lett. **47**, 910 (1981)
36. Grischkowsky, D., Balant, A.C.: Optical pulse compression based on enhanced frequency chirping. Appl. Phys. Lett. **41**, 1–3 (1982)
37. Nakazawa, M., Kubota, H., Suzuki, K., Yamada, E., Sahara, A.: Recent progress in soliton transmission technology. Chaos **10**, 486–514 (2000)
38. Lakoba, T.I., Kaup, D.J.: Hermite–Gaussian expansion for pulse propagation in strongly dispersion managed fibers. Phys. Rev. E **58**, 6728 (1998)
39. Ma, W.X., Chen, M.: Direct search for exact solutions to the nonlinear Schrödinger equation. Appl. Math. Comput. **215**(8), 2835–2842 (2009)
40. Yan, Z., Dai, C.: Optical rogue waves in the generalized inhomogeneous higher-order nonlinear Schrödinger equation with modulating coefficients. J. Opt. **15**, 064012 (2013)
41. Li, J., Zhang, H.Q., Xu, T., Zhang, Y.X., Tian, B.: Soliton-like solutions of a generalized variable-coefficient higher order nonlinear Schrödinger equation from inhomogeneous optical fibers with symbolic computation. J. Phys. A **40**, 13299 (2007)
42. Feng, Y.J., Gao, Y.T., Sun, Z.Y., Zuo, D.W., Shen, Y.J., Sun, Y.H., Yu, X.: Anti-dark solitons for a variable-coefficient higher-order nonlinear Schrödinger equation in an inhomogeneous optical fiber. Phys. Scr. **90**, 045201 (2015)
43. Yang, R., Li, L., Hao, R., Li, Z., Zhou, G.: Combined solitary wave solutions for the inhomogeneous higher-order nonlinear Schrödinger equation. Phys. Rev. E **71**, 036616 (2005)
44. Hao, R., Li, L., Li, Z., Zhou, G.: Exact multisoliton solutions of the higher-order nonlinear Schrödinger equation with variable coefficients. Phys. Rev. E **70**, 066603 (2004)
45. Tian, B., Gao, Y.T., Zhu, H.W.: Variable-coefficient higher-order nonlinear Schrödinger model in optical fibers: variable-coefficient bilinear form, Bäcklund transformation, brightons and symbolic computation. Phys. Lett. A **366**, 223–229 (2007)
46. Meng, X.H., Zhang, C.Y., Li, J., Xu, T., Zhu, H.W., Tian, B.: Analytic multi-solitonic solutions of variable-coefficient higher-order nonlinear Schrödinger models by modified bilinear method with symbolic computation. Z. Naturforsch. A **62**, 13–20 (2007)

47. Dai, C.Q., Zhang, J.F.: New solitons for the Hirota equation and generalized higher-order nonlinear Schrödinger equation with variable coefficients. J. Phys. A **39**, 723 (2006)
48. Bagrov, V.G., Samsonov, B.F.: Darboux transformation of the Schrödinger equation. Phys. Part. Nucl. **28**, 374–397 (1997)
49. Pina, J., Abueva, B., Goedde, C.G.: Periodically conjugated solitons in dispersion-managed optical fiber. Opt. Commun. **176**, 397–407 (2000)
50. Gedalin, M., Scott, T.C., Band, Y.B.: Optical solitary waves in the higher order nonlinear Schrödinger equation. Rev. Lett. **78**, 448 (1997)
51. Li, Z., Li, L., Tian, H., Zhou, G.: New types of solitary wave solutions for the higher order nonlinear Schrödinger equation. Phys. Rev. Lett. **84**, 4096 (2000)
52. Karpman, V.I.: The extended third-order nonlinear Schrödinger equation and Galilean transformation. Eur. Phys. J. B **39**, 341–350 (2004)
53. Annou, K., Annou, R.: Dromion in space and laboratory dusty plasma. In: 2012 Abstracts IEEE International Conference on Plasma Science (ICOPS), p. 2P-19. IEEE
54. Lou, S.Y.: Dromion-like structures in a (3+ 1)-dimensional KdV-type equation. J. Phys. A **29**, 5989 (1996)
55. Hietarinta, J., Hirota, R.: Multidromion solutions to the Davey-Stewartson equation. Phys. Lett. A **145**, 237–244 (1990)
56. Yoshida, N., Nishinari, K., Satsuma, J., Abe, K.: Dromion can be remote-controlled. J. Phys. A **31**, 3325 (1998)
57. Gilson, C.R., Macfarlane, S.R.: Dromion solutions of noncommutative Davey-Stewartson equations. J. Phys. A **42**, 235202 (2009)
58. Zhong, W.P., Belic, M.R., Xia, Y.: Special soliton structures in the (2+ 1)-dimensional nonlinear Schrödinger equation with radially variable diffraction and nonlinearity coefficients. Phys. Rev. E **83**, 036603 (2011)
59. Wong, P., Pang, L.H., Huang, L.G., Li, Y.Q., Lei, M., Liu, W.J.: Dromion-like structures and stability analysis in the variable coefficients complex Ginzburg–Landau equation. Ann. Phys. **360**, 341–348 (2015)
60. Ma, W.X., Qin, Z., Lü, X.: Lump solutions to dimensionally reduced p-gKP and p-gBKP equations. Nonlinear Dyn. **84**(2), 923–931 (2016)
61. Hirota, R.: Exact solution of the Korteweg-de Vries equation for multiple collisions of solitons. Phys. Rev. Lett. **27**, 1192 (1971)
62. Zwillinger, D.: Handbook of Differential Equations, 3rd edn. Academic press, Boston (1997)